Korean J. Chem. Eng., 33(11), 3141-3148 (2016)
DOI: 10.1007/s11814-016-0177-4

pISSN: 0256-1115
eISSN: 1975-7220

Efficient removal of methylene blue in aqueous solution by freeze-dried calcium alginate beads

Guangxue Liu*, Zonggao Hu*, Rouwen Guan*, Yafei Zhao*,†, Hongsong Zhang,†, and Bing Zhang***

*School of Chemical Engineering, Zhengzhou University, Zhengzhou 450001, P. R. China
**Henan Institute of Engineering, Zhengzhou 451191, P. R. China
(*Received 1 December 2015 • accepted 24 June 2016*)

Abstract−Novel porous calcium alginate beads were prepared via crosslinking of calcium followed by freeze drying for investigating the adsorption performance for methylene blue. These beads possessed reduced shrinkage, highly porous lamellar structure and high specific surface area, and exhibited enhanced adsorption capacity and much faster adsorption rate compared to the non-porous beads obtained with conventional oven drying method. Methylene blue adsorption capacity increased with increasing of initial concentration and pH, while decreased with increasing of temperature. The adsorption process fitted well with the pseudo-second-order kinetic model and the Langmuir isotherm. The maximum adsorption capacity was 961.5 mg g^{-1} at 298.15 K. After eight successive adsorption-desorption cycles, the adsorption capacity had negligible decrease. Owing to the high adsorption capability, rapid adsorption rate, easy recovery and reusability, the freeze-dried beads imply a prospective, biodegradable and attractive adsorbent for removing contaminants from wastewater.

Keywords: Adsorption Capacity, Calcium Alginate Beads, Freeze Drying, Methylene Blue, Reusability

INTRODUCTION

Dyes are widely used in a large variety of industries, such as food, plastics, leather, paper, rubber, mineral processing, pharmaceutical, cosmetics, and textile [1,2]. Discharging of colored effluents into waters causes environmental problems due to its seriously harmful effects on environment and life [3]. Dyes mostly have complex and stable structure against sunlight and oxidizing agents, making them hard to degrade by chemical and biological methods. Even if they are degraded, the degradation products still offer serious threats to the marine and inland life. Besides, the undesired color not only affects the aesthetic of the waters but also disrupts the ecological balance by hindering light penetration [4,5]. Thus, it is of great significance to remove them from industrial effluents before discharge.

A variety of methods have been employed to decontaminate wastewater, including reverse osmosis, photodegradation, biochemistry and electrochemistry, ion exchange, and adsorption etc [6,7]. Among them, adsorption is one of the most effective due to low cost, the availability of abundant adsorbents and large capacity of disposal [8]. The commonly used adsorbents are natural zeolites [9], polymers [10], activated carbon [11], clays [12], fly ash [13], and agricultural wastes [14]. However, each have their own different weakness, such as low efficiency, high operating costs, difficult regeneration and secondary pollution.

In the past few years, alginate, a natural polysaccharide extracted from brown algal species which is built up of α-L-guluronic (G) and 1,4 linked β-D-mannuronic acid (M), has gained great research interest for its gelling and metal binding properties. Having advantages such as biodegradability, hydrophilic properties, environmental friendliness, low cost, and abundance combined with its ability to form stable hydrogels due to the presence of specially coordinated carboxylic binding sites for metal, alginate has been widely recognized as ideal support for the immobilization of enzymes and living cells, or as absorbent for contaminants removal from wastewater. However, conventional oven-, air- or vacuum-dried alginate beads have the disadvantages of shrinkage, rigidness, tight nonporous structure, and low diffusion coefficient, resulting in slow adsorption kinetics and lower adsorption capacity [15]. Indeed, as reported [16], the main drawback of conventionally dried alginate bead as absorbent is low porosity, since it delays molecular diffusion in the particle interior. Therefore, using the same material in porous form could probably improve its adsorption kinetics and isotherm properties. Freeze drying, on the other hand, is an attractive method to form porous beads based on sublimation, which has a wide application in the pharmaceutical and food industries. It has the ability to rapidly freeze the solution to ice and then transform ice to vapor without passing through the liquid phase under high vacuum condition, resulting in porous form that possesses a controllable morphology and high specific surface area [17-19]. Such porous form has already attracted considerable attention and extensive use in catalysis, food, hydrocarbon adsorption, and biomedicine due to its unique three-dimensional network structure, low density, high surface area, high porosity, and high storage capacity [15]. However, no previous studies have been reported to utilize freeze-dried alginate beads as adsorbents for dyes removal from wastewater.

We report here the synthesis of novel porous calcium alginate

†To whom correspondence should be addressed.
E-mail: zhaoyafei007@126.com, zhsandchen@126.com

beads through simple calcium crosslinking followed by freeze drying. The freeze-dried beads were characterized and tested for methylene blue adsorption. The parameters influencing the adsorption capacity, including contact time, pH, initial concentration and temperature, were investigated. The adsorption kinetics and equilibrium isotherms were also evaluated and compared with those of the oven-dried alginate beads.

MATERIALS AND METHODS

1. Materials

Alginate (chemical grade) was obtained from Paini Chemical Reagent Co., Ltd. (Zhengzhou, China). Methylene blue and anhydrous calcium chloride (analytical grade) were purchased from Fuchen Chemical Reagent Co., Ltd. (Tianjin, China). The experimental solutions were prepared by dissolving accurately weighed methylene blue into distilled water for different initial concentrations. The initial pH of methylene blue solution was adjusted with 0.1 M HCl and 0.1 M NaOH. All other chemicals were analytical grade and used without further purification.

2. Instrumentation and Characterization

FTIR spectra were recorded with KBr pellet in the range of 400-4,000 cm^{-1} by using a Nicolet Nexus 470 spectrophotometer. The surface areas of the freeze-dried and oven-dried beads were determined from the N_2 adsorption isotherm at 77 K by Multipoint Brunauer-Emmett-Teller (MBET) instrument (NOVA4200e, USA). The micromorphology and nanostructures of samples were investigated using JSM-7500F scanning electron microscope (SEM).

3. Preparation of Freeze-dried Calcium Alginate Beads

4 g of sodium alginate was slowly added into 45 mL of distilled water in a beaker under magnetic stirring, and the mixed solution was continued stirring for 3 h at room temperature to obtain a thick homogenous liquid. The mixture was left there for another 2 h to allow the air to dissipate and bubbles to release from the gel solution. Then, the mixture was slowly dropped into 2% (m/V) calcium chloride solution by a 20 mL medical syringe under continuous stirring. The formed hybrid beads were left in the solution for 24 h to make sure they ripened and then were filtered and washed for several times with distilled water to remove residual calcium chloride. Finally, the gel beads were directly soaked into liquid nitrogen to stand for 10 min and then transferred to a freeze-dryer under a reduced pressure of 10-20 Pa for 12 h to obtain freeze-dried calcium alginate beads. As comparison, the oven-dried alginate beads were also prepared by drying the gel beads in an oven at 40 °C for 12 h.

4. Adsorption and Regeneration Experiments

The batch adsorption experiments were carried out in 50 mL conical flasks containing 0.05 g of samples and 30 mL of methylene blue solutions of desired concentration. Then, the flasks were shaken in an HZQ-F100-temperature oscillation incubator (Taicang, China) with shaking speed of 140 rpm and setting temperature to reach equilibrium on dye adsorption. The initial and final methylene blue concentrations remaining in solutions were analyzed using a UV spectrophotometer (Shimadzu, UV-3000) by monitoring the absorbance changes at a wavelength of maximum absorbance (663 nm). The adsorption capacity (q_t) at any time was calculated by the following equation:

$$q_t = \frac{(C_0 - C_t)V}{m} \quad (1)$$

where V is the volume of the dye solution (L), and m is the amount of adsorbents (g), C_0 and C_t represent the initial dye concentration (mg L^{-1}) and the dye concentration at any time (mg L^{-1}), respectively.

To study the reusability of the freeze-dried alginate beads, the used adsorbents were desorbed in the mixed solution of anhydrous ethanol and hydrochloric acid (0.1 M) (volume ratio 1 : 1) in a flask and then shaken in an incubator for 10 minutes followed by filtration and wash with deionized water. The above procedure was repeated several times until the eluent was colorless. Finally, the samples were dried in the air and reused as adsorbents.

RESULTS AND DISCUSSION

1. Characterization

Digital photographs were taken to study the surface morphologies of freeze-dried and oven-dried calcium alginate beads, as shown in Fig. 1. It can be seen that wet alginate hydrogel beads have a smooth and uniform surface with the average diameter of about 3.3 mm (Fig. 1(a)). After freeze drying, no obvious changes can be observed, and alginate beads could perfectly keep their shape with slight decrease in diameter to 3.0 mm (Fig. 1(b)). However, a heterogeneous and rough surface caused by numerous bulges on the oven-dried beads is observed. The diameter reduces significantly to 0.2 mm and the surface of oven-dried beads becomes shriveled, indicating serious deformation after oven drying (Fig. 1(c)).

To investigate the interior structure, the cross-section morphol-

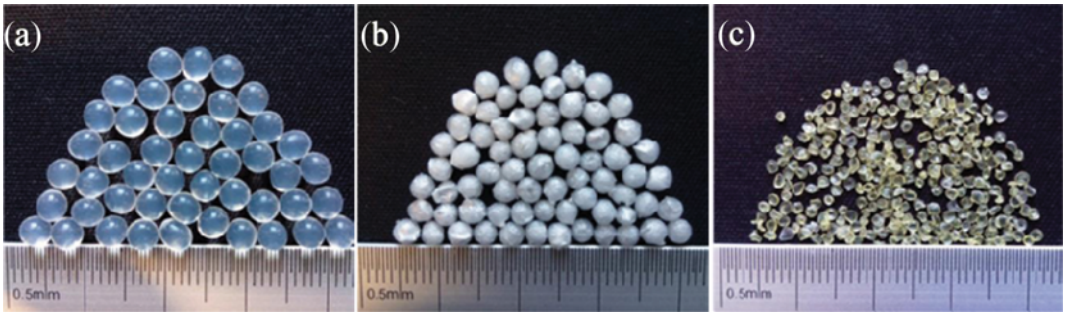

Fig. 1. Photographs of calcium alginate hydrogel beads (a), freeze-dried beads (b), and oven-dried beads (c).

ogies of the freeze-dried beads and oven-dried beads were characterized by SEM (Fig. 2). As clearly observed in Fig. 2, freeze-dried calcium alginate beads possess macroporous structure constructed by a series of loose layers with irregular shapes (Fig. 2(a), (b)), while oven-dried beads have very dense structure with no pores presence at all (Fig. 2(c), (d)). As noted previously, porous structure is an important factor for enhancing adsorption rate and uptakes of adsorbate by providing more accessible active site directly and allowing fast ion diffusion. In this case, freeze-dried alginate beads may offer better adsorption performance than the oven-dried beads.

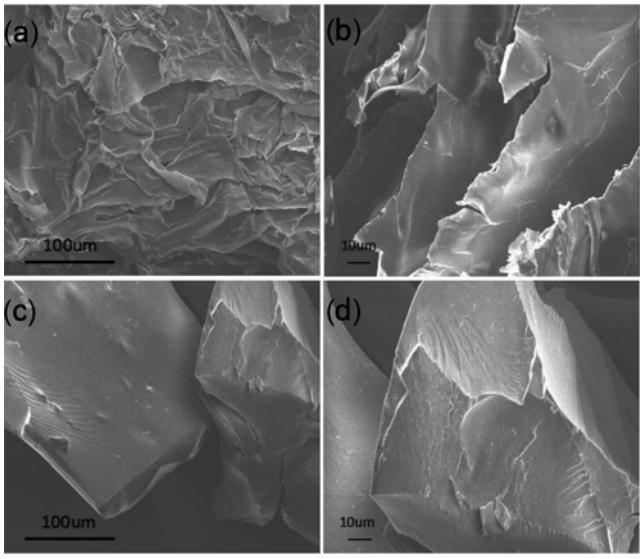

Fig. 2. SEM images of the cross-section of freeze-dried calcium alginate beads (a), (b) and oven-dried beads (c), (d).

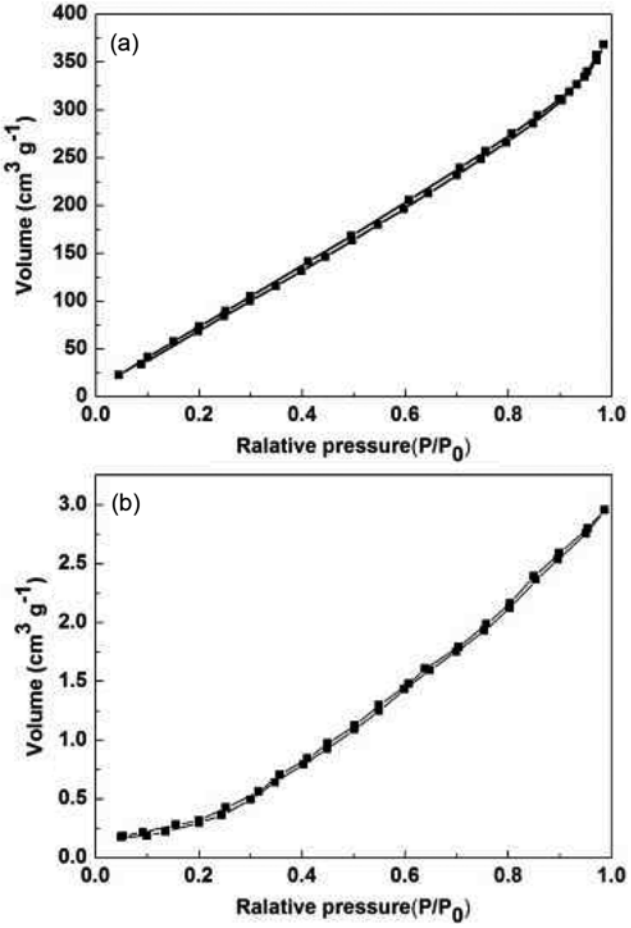

Fig. 3. N_2 adsorption-desorption isotherms of the freeze-dried calcium alginate beads (a) and oven-dried beads (b).

BET analysis for the specific surface area was performed to better understand the particular physical process that might take place within the adsorbents. N_2 adsorption-desorption isotherms (Type III) of the obtained samples are shown in Fig. 3, revealing that the beads possessed a macroporous structure or dense structure with no pores. Freeze-dried alginate beads have more than one-hundred-and-eighty times higher surface area than that of the oven-dried beads (461.46 vs. 2.486 $cm^2 g^{-1}$), indicating that the freeze-dried beads have macroporous structure, whereas the oven-dried beads almost have no pores, which is consistent with the result of SEM. Generally, large specific surface area is beneficial to pollutant removal by increasing the contact frequency between the pollutants and adsorbents. Moreover, the adsorption performance of adsorbent is also highly dependent on the internal pore structure [20,21]. Large pore structure (e.g., macroporosity) can promote the transfer of the material, which is advantageous to pollutant adsorption or entrapment.

2. Adsorption Comparison of Freeze-dried and Oven-dried Beads

In this study, 0.05 g of different samples were added into 30 mL of methylene blue solutions with initial concentrations of 500 mg L^{-1}, respectively. The adsorption behaviors of freeze-dried and oven-dried beads are shown in Fig. 4. Notably, an increase in maximum adsorption capacity can be observed for freeze-dried beads compared to the oven-dried beads, although they are prepared from the same material containing the same number of active sites. This can be attributed to the influence of mainly stereochemical factors. It is possible that the rigid and tight polymeric structure of oven-dried beads may prevent ions from reaching the Ca^{2+} for rearrangement, hence making some adsorption sites inaccessi-

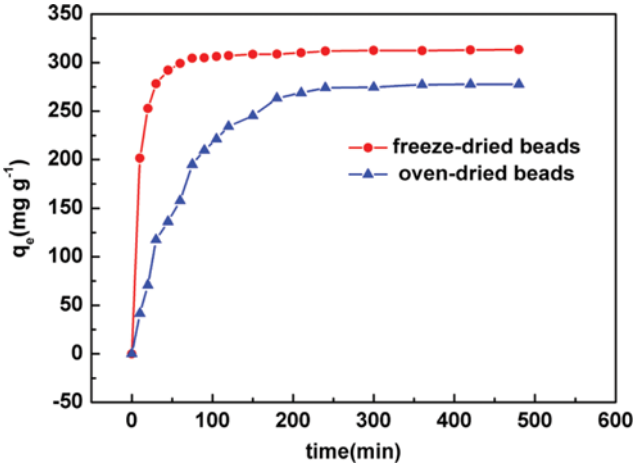

Fig. 4. Adsorption comparison of the freeze-dried and oven-dried beads.

ble [15]. However, freeze-dried beads with higher surface area and higher porous volume can diminish this hindering effect and result in increased site accessibility and higher occupation percentage for methylene blue. Besides, the adsorption for freeze-dried beads approaches equilibrium after 60 min and no significant increase in methylene blue adsorption is observed after that time, while the equilibrium is approached in 240 min for the oven-dried beads. Steric hindrance and surface area could also explain the faster kinetics of the freeze-dried beads than the oven-dried beads [15].

3. Adsorption Kinetics

To yield further information on the mechanisms involved, batch experiments were carried out to study the adsorption kinetics which predicate the rate of adsorption and control the time of equilibrium adsorption. The kinetics of adsorption process were tested with the Lagergren pseudo-first-order [22] and pseudo-second-order kinetic models [23], which can be expressed in the following equations, respectively:

$$\log(q_e - q_t) = \log q_e - \frac{k_1 t}{2.303} \quad (2)$$

$$\frac{t}{q_t} = \frac{1}{k_2 q_e^2} + \frac{1}{q_e} t \quad (3)$$

where k_1 (min^{-1}) is the rate constant of the first-order kinetic model and k_2 (min^{-1}) is the rate constant for the pseudo-second-order adsorption process, q_e and q_t are the quantities of dye adsorbed at equilibrium and at given time t (mg g^{-1}), respectively. k_1, k_2 and q_e can be calculated from the slope and intercept of the plot, respectively.

Fitting of both kinetics models and the derived kinetic parameters for the freeze-dried alginate beads at different initials concentrations are presented in Fig. 5 and Table 1. Note that all the experiment data lie on the pseudo-second-order kinetic line, but some of them keep away from pseudo-first-order kinetic line, indicating better fitness for the pseudo-second-order kinetic model (Fig. 5). Also, the calculated values of q_{1e} fail to predicate the values of q_{exp}, while the values of q_{2e} are fairly close to q_{exp}, and the correlation coefficients obtained from pseudo-second-order equation are larger than 0.999, which further suggests that the entire adsorption process of the freeze-dried beads obeys the pseudo-second-order kinetic model (Table 1). This indicates that the adsorption for alginate is mainly dependent on chemical adsorption involving valent forces through sharing or exchanging of electrons between the adsorbent and methylene blue.

4. Adsorption Influencing Factors

4-1. Effect of Contact Time

The uptake of methylene blue versus contact time at different initial dye concentrations (400, 500 and 600 mg L^{-1}) is presented in Fig. 6. The adsorption capacity increased with contact time increasing, and the adsorption rate was very high in the first 30 min and finally equilibrium was attained in 60 min. The rapid adsorption was probably related to the availability of free adsorption sites on the freeze-dried beads surface in the initial stage. Adsorption became less efficient with the gradual occupancy of active sites, and the equilibrium was reached after saturation of the available sites. Particularly noteworthy is the speed of the adsorption for the three initial concentrations. The initial rate of the adsorption is greater for higher initial methylene blue concentration because the resistance to the dye uptake diminishes and the mass transfer driving force increases [24]. The adsorption capacity increases from 222.8 mg g^{-1} to 360.5 mg g^{-1} with the initial concentration of meth-

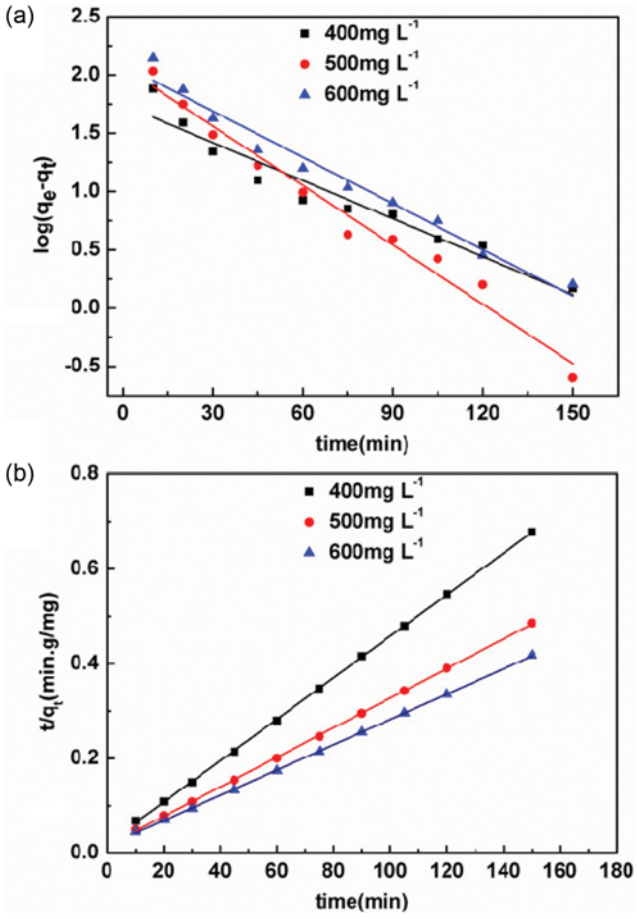

Fig. 5. Pseudo-first-order (a) and pseudo-second-order (b) kinetic plots for methylene blue adsorption onto the freeze-dried beads.

Table 1. Adsorption Kinetic Parameters of methylene blue onto the freeze-dried alginate beads

Models		Pseudo-first-order			Pseudo-second-order		
C_0 (mg L^{-1})	$q_{e,exp}$ (mg g^{-1})	$-k_1\times10^{-2}$ (min^{-1})	$q_{1e,cal}$ (mg g^{-1})	R^2	$k_1\times10^{-2}$ (min^{-1})	$q_{2e,cal}$ (mg g^{-1})	R^2
400	222.8	1.085	55.60	0.9322	0.438	228.3	0.9998
500	308.9	1.696	117.2	0.9750	0.312	320.5	0.9998
600	360.5	1.320	121.9	0.9709	0.267	374.5	0.9998

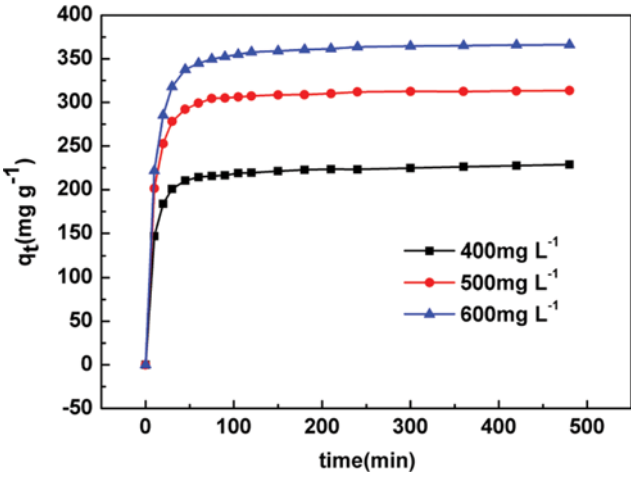

Fig. 6. Effect of contact time for methylene blue onto the freeze-dried beads.

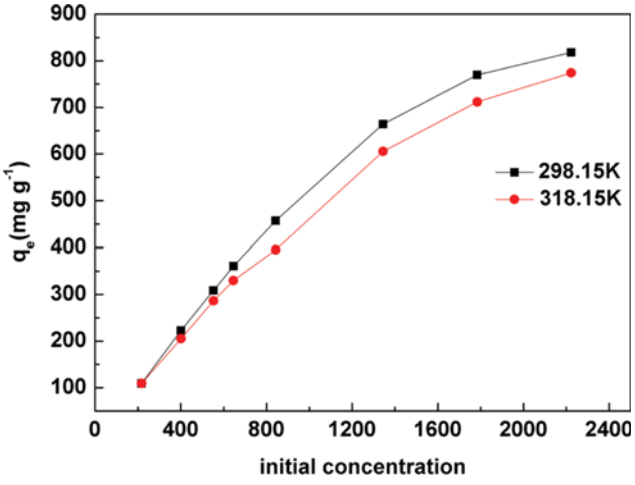

Fig. 7. Effect of initial concentration and temperature for methylene blue adsorption onto the freeze-dried alginate beads.

ylene blue changing from 400 mg L^{-1} to 600 mg L^{-1}; this could be attributed to greater driving force resulting from greater concentration gradient between aqueous solution and adsorbent surface at higher initial dye concentration [25].

4-2. Effect of Initial Concentration and Temperature

Batch adsorption experiments with varied initial methylene blue concentrations were conducted to explore the effect of initial concentration at 298.15 and 318.15 K for 60 min. Fig. 7 shows that the adsorption capacity of the freeze-dried beads increases with the increase of initial concentrations. The higher initial dye concentration provides greater driving force, which is beneficial to the mass transfer of methylene blue from the aqueous solution to solid surface [26]. The equilibrium adsorption capacity could reach 818.01 mg g^{-1} when the initial methylene blue concentration is 2,200 mg L^{-1} at 298.15 K. Temperature also plays an important role in the adsorption process; the adsorption capacity was found to decrease with increase of temperature, indicating the process is exothermic.

4-3. Effect of Initial pH

The pH of the aqueous solution is an important controlling

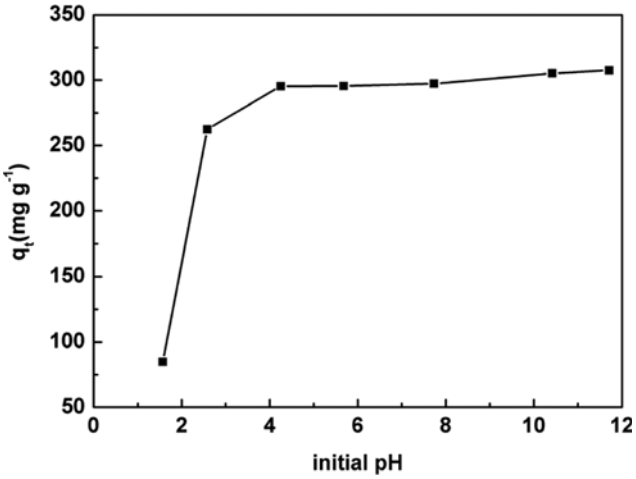

Fig. 8. Effect of pH on the methylene blue adsorption onto the freeze-dried beads.

parameter due to its impact on both the surface active sites of the adsorbents and the ionization process of the dye molecules in the adsorption process [27]. Various pH values (1.5-12) of methylene blue aqueous with the initial concentration of 500 mg L^{-1} were studied at 298.15 K and the results are illustrated in Fig. 8. It can be seen that the equilibrium adsorption capacity has a sharp increase with the increase of pH values from 1.5 to 4, while no significant alteration in the pH range of 4-12. When pH value is lower than 4, the carboxylate groups on the polymeric chains may convert to the carboxylic acid groups, which weakens the electrostatic attraction between the freeze-dried alginate beads and methylene blue, and thus the adsorption capacity is decreased with the decrease of pH. When pH was increased to 4-12, the deprotonation of the carboxylic acid generated more negatively charged absorption sites in the hydrogel to enhance the adsorption capacity. Besides, the presence of excess of H^+ ions at low pH will compete with the dye cations for adsorption sites, resulting in a decrease in the adsorption capacity, while more negatively charged surface of the adsorbents becomes available with the increasing pH value [28]. This adsorption behavior of the freeze-dried calcium alginate beads at various pHs suggests that they can be potentially applied in a wide pH range.

5. Equilibrium Adsorption Isotherm

Adsorption isotherm models are widely used to describe the adsorption process and investigate mechanisms of adsorption. The equilibrium data was analyzed by the Langmuir and Freundlich isotherm models. The Langmuir isotherm is derived and developed from the assumption that the adsorbent surface can only occur at the surface monolayer homogeneously [29] and there is no interaction between the adsorbate molecules:

$$\frac{C_e}{q_e} = \frac{1}{q_{max} K_L} + \frac{C_e}{q_{max}} \quad (4)$$

where C_e is the equilibrium concentration of methylene blue in solution (mg L^{-1}), K_L is the Langmuir binding constant, q_e and q_{max} are the amounts of methylene blue (mg g^{-1}) adsorbed at equilibrium and maximum adsorption capacity (mg g^{-1}), respectively.

Plotting C_e/q_e versus C_e gives a straight line, q_{max} and K_L can be calculated from the slope ($1/q_{max}$) and intercept ($1/q_{max}K_L$). To estimate whether the adsorption process is favorable or unfavorable, a dimensionless constant separation factor or equilibrium parameter R_L is defined according to the following equation:

$$R_L = \frac{1}{1+K_L C_0} \quad (5)$$

Here, the R_L value reveals the type of the isotherm to be either favorable or unfavorable. When the $R_L>1$, it is considered as an unfavorable process; $R_L<0$ indicates the adsorption process is irreversible; when $0<R_L<1$, it is conducive to adsorption [30].

The Langmuir plots for methylene blue adsorption onto the freeze-dried beads are obtained in Fig. 9, and the parameters are shown in Table 2. Both of the correlation coefficients of the isotherms are higher than 0.999 at the two temperatures, thereby indicating that the Langmuir isotherm fits the equilibrium data very well. The values of q_{max} for the freeze-dried beads decrease with increasing temperature, indicating the adsorption process is exothermic. The maximum monolayer adsorption capacities are 961.5 mg g^{-1} at 298.15 K and 917.4 mg g^{-1} at 318.15 K, respectively. The calculated values of R_L lie in the range of 0-1, thereby confirming that both of the adsorption processes are favorable. These results

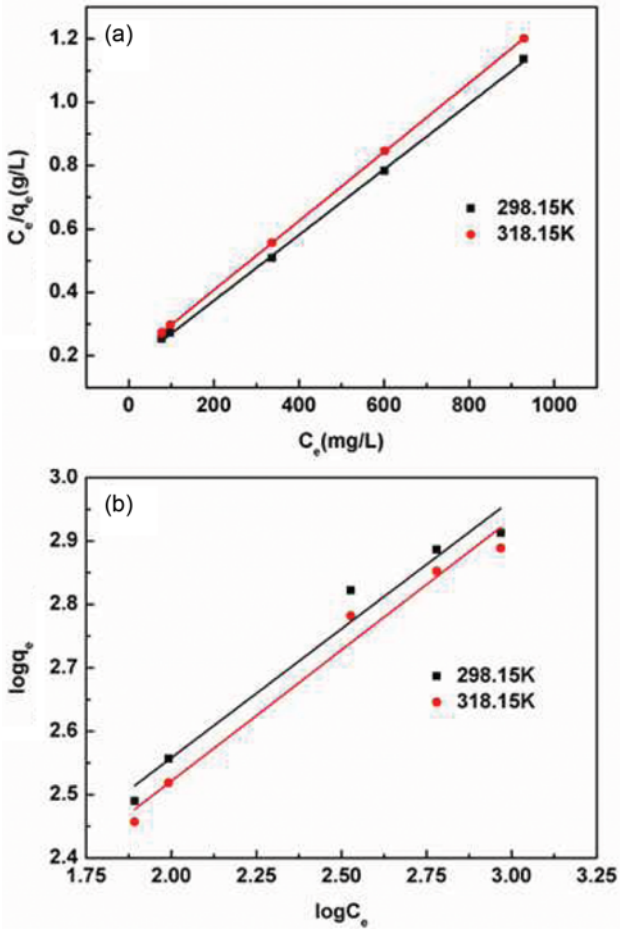

Fig. 9. Langmuir (a) and Freundlich (b) plots for the methylene blue adsorption onto the freeze-dried calcium alginate beads.

Table 2. Isotherm parameters for the methylene blue adsorption onto the freeze-dried alginate beads

Isotherm models	Temperature (K)	
	298.15	318.15
Langmuir		
q_{max} (mg g^{-1})	961.5	917.4
K_L	0.00624	0.00576
R_L (L mg^{-1})	0.06727-0.2248	0.07246-0.2391
R^2	0.9995	0.9999
Freundlich		
1/n	0.4166	0.4134
K_f ($mg^{1-1/n}\cdot L^{1/n}\cdot g^{-1}$)	55.55	49.49
R^2	0.9591	0.9715

demonstrate that the surface of the freeze-dried alginate beads is homogeneous and a monolayer of methylene blue covers the surface after adsorption.

The Freundlich isotherm applies to nonideal adsorption (multilayer adsorption) on a heterogeneous adsorbent surface [31], which is presented in the following equation:

$$\log q_e = \log K_f + \frac{1}{n}\log C_e \quad (6)$$

where C_e is the equilibrium concentration of methylene blue in solution (mg L^{-1}). q_e is the equilibrium adsorption capacity (mg g^{-1}) of methylene blue, K_f is the Freundlich binding constant, and 1/n is an empirical constant related to adsorption intensity. Higher value for K_f indicates higher affinity for adsorbate and the values of the empirical parameter 1/n lie between $0.1<1/n<1$, indicating favorable adsorption [32]. Freundlich constants are calculated from the slope and intercept in Fig. 9(b) and are given in Table 2. The correlation coefficients ($R^2>0.95$) reflect that the experimental data agree with the Freundlich model, suggesting multilayer adsorption is involved in the adsorption process. The values of 1/n 0.4166, and 0.4134 at 298.15 and 318.15 K are both smaller than 1, so they represent the favorable removal conditions.

6. Regeneration and Reuse of the Freeze-dried Calcium Alginate Beads

Reusability of an adsorbent is of critical significance in practical applications for dye removal from wastewaters. Regeneration experiments were performed by eluting the used adsorbents with mixed solution of anhydrous ethanol and hydrochloric acid (0.1 M), and reused them in the adsorption and desorption processes to explore the potential reutilization of the freeze-dried calcium alginate beads as adsorbents for methylene blue (500 mg L^{-1}) removal from aqueous solutions. The results are illustrated in Fig. 10. Clearly, the adsorption capacities basically remain unchanged after undergoing eight times of adsorption/desorption cycles, meaning the excellent reusability of the freeze-dried alginate beads. It is concluded that the adsorbent can be regenerated easily using the eluent under the normal temperature and pressure. Consequently, the freeze-dried calcium alginate beads can be considered as reusable absorbents.

7. Adsorption Mechanism

To understand the adsorption mechanism further, the FTIR

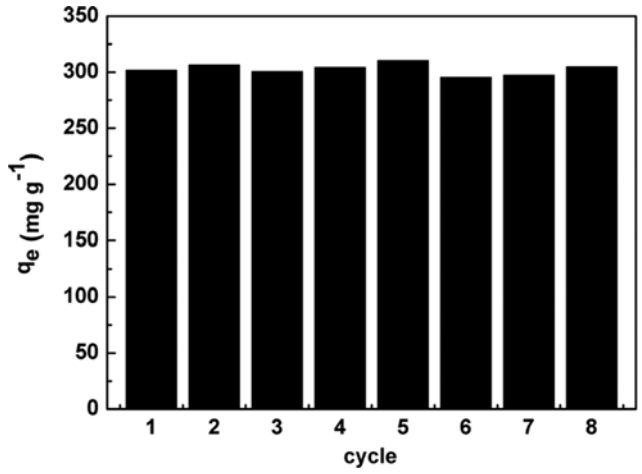

Fig. 10. The regeneration of the freeze-dried calcium alginate beads.

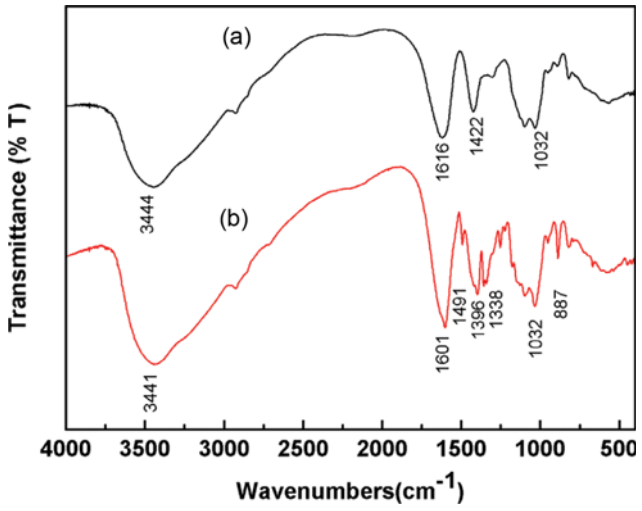

Fig. 11. FTIR spectra of the freeze-dried calcium alginate beads before (a) and after (b) methylene blue adsorption.

spectra of the freeze-dried calcium alginate beads before and after adsorption of methylene blue are shown in Fig. 11. As shown in Fig. 11(a) for the freeze-dried beads, the broad and intense band observed at 3,444 cm^{-1} is ascribed to the stretching vibration of OH, while the peak at 1,616 cm^{-1} is responsible for the C=O stretching vibration of the COOH groups. The peaks at 1,423 and 1,032 cm^{-1} belong to the vibration of C-H bonds in alkanes and C-O-C stretching vibration, respectively. The results indicate that the freeze-dried calcium alginate beads possess carbonyl and hydroxyl functional groups, which are active binding groups to effectively capture methylene blue from aqueous solution. After the adsorption of methylene blue onto the freeze-dried calcium alginate beads (Fig. 11(b)), the beads keep most of their characteristic peaks, indicating that physical adsorption is involved in the adsorption process. Additionally, on one hand, many functional groups shift to different bands. The bands at 3,444 and 1,616 cm^{-1} transferred to lower frequencies at 3,441 and 1,601 cm^{-1}, respectively, whereas the peak at 1,422 cm^{-1} disappears after adsorption, attributed to the interaction of hydroxyl and carboxyl groups from alginate with $N(CH_3)^{2+}$ group on methylene blue molecules. On the other hand, the obvious new bands at 1,491, 1,338 and 887 cm^{-1} correspond to aromatic skeletal C=C stretching vibrations, C-N stretching vibrations and C-H deformation vibrations in arene, respectively, which belong to methylene blue molecules. The shift, disappearance and appearance of different active functional groups on the freeze-dried calcium alginate beads after adsorption indicate the possible interaction of surface sites with methylene blue molecules, implying that electrostatic attraction between negatively charged freeze-dried alginate beads and positively charged methylene blue also plays an important role in the adsorption.

CONCLUSION

Highly porous freeze-dried calcium alginate beads were fabricated and investigated as adsorbents to remove methylene blue from aqueous solutions. The freeze-dried alginate beads possess reduced shrinkage, porous laminar structure and higher surface area, and exhibit higher adsorption capacity and adsorption rate compared with oven-dried beads. The adsorption capacity of methylene blue increased with increasing the contact time, pH value and initial concentration, but the increase of temperature was unfavorable for adsorption. Pseudo-second-order model depicted the adsorption kinetics satisfactorily, and the Langmuir isotherm was a better fitted model for the adsorption of methylene blue. The maximum adsorption capacity can reach as high as 961.5 mg g^{-1} at 298.15 K and the freeze-dried calcium alginate beads can be easily regenerated and reused. Electrostatic attraction between carboxylate groups and methylene blue dominated the whole adsorption process. The obtained results reveal that the freeze-dried calcium alginate beads can be attractive adsorbents for dye removal from aqueous solution.

ACKNOWLEDGEMENTS

This work was supported by the National Natural Science Foundation of China (No. 20871105 and 21576247) and Postdoctoral Research Sponsorship of Henan Province (Grant No. 2015015).

NOMENCLATURE

Symbols

C_e : equilibrium concentration of methylene blue in solution [mg L^{-1}]
C_0 : initial dye concentration [mg L^{-1}]
C_t : dye concentration at any time [mg L^{-1}]
K_f : Freundlich binding constant
K_L : Langmuir binding constant
k_1 : rate constant of the first order kinetic model [min^{-1}]
k_2 : rate constant of the pseudo-second-order kinetic model [min^{-1}]
m : amount of adsorbents [g]
1/n : empirical constant related to adsorption intensity
q_e : equilibrium adsorption capacity of methylene blue [mg g^{-1}]
q_{max} : maximum adsorption capacity of methylene blue [mg g^{-1}]
q_t : quantities of dye adsorbed at given time t [mg g^{-1}]

R_L : dimensionless constant separation factor or equilibrium parameter
V : volume of the dye solution [L]

REFERENCES

1. E. N. El Qada, S. J. Allen and G. M. Walker, *J. Chem. Eng.*, **124**, 103 (2006).
2. A. F. Alkaim, Z. Sadik, D. K. Mahdi, S. M. Alshrefi, A. M. Al-Sammarraie, F. M. Alamgir, P. M. Singh and A. M. Aljeboree, *Korean J. Chem. Eng.*, **32**, 2456 (2015).
3. M. Shirmardi, A. H. Mahvi, B. Hashemzadeh, A. Naeimabadi, G. Hassani and M. V. Niri, *Korean J. Chem. Eng.*, **30**, 1603 (2013).
4. X. He, K. B. Male, P. N. Nesterenko, D. Brabazon, B. Paull and J. H. Luong, *ACS Appl. Mater. Interfaces*, **5**, 8796 (2013).
5. B. H. Hameed and A. A. Ahmad, *J. Hazard. Mater.*, **164**, 870 (2009).
6. S. Arabi and M. R. Sohrabi, *Water Sci. Technol.*, **70**, 24 (2014).
7. R. Zhai, B. Zhang, Y. Wan, C. Li, J. Wang and J. Liu, *Chem. Eng. J.*, **214**, 304 (2013).
8. L. Liu, Y. Wan, Y. Xie, R. Zhai, B. Zhang and J. Liu, *Chem. Eng. J.*, **187**, 210 (2012).
9. D. Karadag, E. Akgul, S. Tok, F. Erturk, M. A. Kaya and M. Turan, *J. Chem. Eng. Data*, **52**, 2436 (2007).
10. R. S. Blackburn, *Environ. Sci. Technol.*, **38**, 4905 (2004).
11. A. L. Serpa, I. A. H. Schneider and J. Rubio, *Environ. Sci. Technol.*, **39**, 885 (2005).
12. F. Fu, Z. Gao, L. Gao and D. Li, *Ind. Eng. Chem. Res.*, **50**, 9712 (2011).
13. M. Ahmaruzzaman, *Energy Fuels*, **23**, 1494 (2009).
14. Y. S. Ho, W. T. Chiu and C. C. Wang, *Bioresour. Technol.*, **96**, 1285 (2005).
15. E. G. Deze, S. K. Papageorgiou, E. P. Favvas and F. K. Katsaros, *Chem. Eng. J.*, **209**, 537 (2012).
16. R. Lagoa and J. R. Rodrigues, *Biochem. Eng. J.*, **46**, 320 (2009).
17. M. D. Eddleston, B. Patel, G. M. Day and W. Jones, *Cryst. Growth Des.*, **13**, 4599 (2013).
18. S. R. Mukai, H. Nishihara, S. Shichi and H. Tamon, *Chem. Mater.*, **16**, 4987 (2004).
19. T. Okada, T. Kato, T. Yamaguchi, T. Sakai and S. Mishima, *Ind. Eng. Chem. Res.*, **52**, 12018 (2013).
20. K. Kosuge, S. Kubo, N. Kikukawa and M. Takemori, *Langmuir*, **23**, 3095 (2007).
21. M. Kruk, M. Jaroniec and A. Sayari, *J. Phys. Chem B.*, **101**, 583 (1997).
22. B. H. Hameed and M. I. El-Khaiary, *J. Hazard. Mater.*, **155**, 601 (2008).
23. Y. S. Ho and G. McKay, *Chem. Eng. J.*, **70**, 115 (1998).
24. C. A. Almeida, N. A. Debacher, A. J. Downs, L. Cottet and C. A. Mello, *J. Colloid Interface Sci.*, **332**, 46 (2009).
25. M. Doğan, M. Alkan, Ö. Demirbaş, Y. Özdemir and C. Özmetin, *Chem. Eng. J.*, **124**, 89 (2006).
26. V. K. Gupta, A. Nayak and S. Agarwal, *Environ. Eng. Res.*, **20**, 1 (2015).
27. D. C. dos Santos, M. A. Adebayo, S. de Fátima Pinheiro Pereira, L. D. T. Prola, R. Cataluña, E. C. Lima, C. Saucier, C. R. Gally and F. M. Machado, *Korean J. Chem. Eng.*, **31**, 1470 (2014).
28. H. Shi, W. Li, L. Zhong and C. Xu, *Ind. Eng. Chem. Res.*, **53**, 1108 (2014).
29. I. Langmuir, *J. Amer. Chem. Soc.*, **38**, 2221 (1916).
30. K. R. Hall, L. C. Eagleton, A. Acrivos and T. Vermeulen, *Ind. Eng. Chem. Fundam.*, **5**, 212 (1966).
31. R. Liu, B. Zhang, D. Mei, H. Zhang and J. Liu, *Desalination*, **268**, 111 (2011).
32. A. S. Ozcan, B. Erdem and A. Ozcan, *J. Colloid Interface Sci.*, **280**, 44 (2004).